Contributions of dark matter annihilation to the global 21 cm spectrum observed by the EDGES experiment

Yupeng Yang

Collage of Physics and Electrical Engineering, Anyang Normal University, Anyang, 455000, China and Joint Center for Particle, Nuclear Physics and Cosmology, Nanjing, 210093, China

(Received 18 March 2018; published 5 November 2018)

The EDGES experiment has observed an absorption feature in the global 21 cm spectrum with a surprisingly large amplitude. These results can be explained by decreasing the kinetic temperature of baryons, which could be achieved through the scattering between the baryons and cold dark matter particles. It seems that the most researched dark matter annihilation model is not able to explain such a large amplitude, since the interactions between the particles produced by the dark matter annihilation and the particles that have been present in the Universe could increase the baryonic temperature. Recently, C. Feng and G. Holder have suggested that the large amplitude in the global 21 cm spectrum could be produced by considering the possible excess of the early radio radiation. In this paper, we propose that the dark matter annihilation still works to explain the large amplitude observed by the EDGES experiment. Even including the dark matter annihilation, the large absorption amplitude in the global 21 cm spectrum can be produced by considering the possible excess of the early radio radiation.

DOI: 10.1103/PhysRevD.98.103503

I. INTRODUCTION

As an important way of exploring the "dark ages" of the Universe, the global 21 cm spectrum has been studied in theory by many works; see, e.g., Refs. [1–3]. Recently, the EDGES experiment reported the observational results on the global 21 cm spectrum, which finds an absorption feature at the redshift $z \sim 17$ with a surprisingly large amplitude $T_{21} \sim 500$ mK [4], twice as large as expected. The global 21 cm spectrum is the result of the competition among the kinetic temperature (T_k), the cosmic microwave background (CMB) thermodynamic temperature ($T_{\rm CMB}$), and the spin temperature (T_s). One possible way of explaining the observed large amplitude is decreasing the kinetic temperature T_k, which could be achieved if the scattering between the baryons and cold dark matter particles is present [5–8]. Another possible way is enhancing the temperature of the cosmic radio background [9–11]. In Ref. [12], the ARCADE-2 experiment reported the excess of the cosmic radio background in the frequency $\nu \lesssim 1$ GHz, and the corresponding temperature can be fitted with a form

$$T(\nu) = T_0 + T_e \left(\frac{\nu}{1\ \text{GHz}}\right)^{\alpha}, \tag{1}$$

where $T_0 = 2.729 \pm 0.004$ K is the CMB thermodynamic temperature at $z = 0$, $T_e = 1.19 \pm 0.14$ K and $\alpha = -2.62 \pm 0.04$. The excess of the cosmic radio background, not explained easily by the standard sources, could be from the early radio sources such as the radio-loud quasars; see, e.g., Refs. [13–17]. Some authors have found that the radio excess could be explained by the dark matter annihilation [18–20].[1] The main point is that the electrons produced during the dark matter annihilation could emit the synchrotron radiation within the cosmic magnetic field. On the other hand, the evolution of the Universe could be influenced by the dark matter annihilation [21–27]. One of the influences is heating the intergalactic medium (IGM) and enhancing the kinetic temperature T_k. Therefore, it seems that the dark matter annihilation is not able to explain the observed large amplitude of the global 21 cm spectrum [28,29]. In Ref. [10], the authors found that the amplitude of the global 21 cm spectrum could reach a very large amplitude, $T_{21} \sim 1100$ mK, even with 10% of the observed radio excess. In this paper, we propose that, although the dark matter annihilation can increase the kinetic temperature, it could still explain the observed large absorption amplitude in the global 21 cm spectrum. Even including the dark matter annihilation, the large absorption amplitude in the global 21 cm spectrum could appear by considering the possible excess of the early radio radiation.

This paper is organized as follows. In Sec. II, we review the basic quantities of the global 21 cm signal. The influences of dark matter annihilation and the first stars on IGM are investigated in Sec. III. In Sec. IV, we investigate the global 21 cm spectrum including the dark

[1] One should notice that the radio excess explained by the dark matter annihilation is observed at $z = 0$.

matter annihilation and the excess of the cosmic radio background. The conclusions and discussions are given in Sec. V.

II. BASIC QUANTITIES OF THE GLOBAL 21 CM SIGNAL

In this section, we briefly review the basic quantities of the global 21 cm signal. For detailed discussions, one can refer to, e.g., Refs. [1–3] and references therein.

The 21 cm signal is accounted for by the transition of the hyperfine split of hydrogen. The ground state of hydrogen can split into triplet and singlet states, and the energy change of the two levels is $E = 5.9 \times 10^{-6}$ eV, corresponding to the wavelength of photon $\lambda = 21$ cm. The spin temperature T_s is defined as

$$\frac{n_1}{n_0} = 3 \exp\left(-\frac{T_\star}{T_s}\right), \tag{2}$$

where n_1 and n_0 are the number densities of hydrogen in triplet and singlet states and $T_\star$ is the equivalent temperature corresponding to the transition energy.

The spin temperature is mainly effected by (i) the background photons, (ii) the collisions of the hydrogen atoms with other particles, and (iii) the resonant scattering of Lyα photons. Including these factors, the spin temperature can be written as [21,22]

$$T_s = \frac{T_{\rm CMB} + (y_\alpha + y_c)T_k}{1 + y_\alpha + y_c}, \tag{3}$$

where y_α corresponds to the Wouthuysen-Field effect, and in this work, we adopt the form used in Refs. [22,30],

$$y_\alpha = \frac{P_{10} T_\star}{A_{10} T_k} \mathrm{e}^{-0.3(1+z)^{0.5} T_k^{-2/3}(1+0.4/T_k)^{-1}}, \tag{4}$$

where $A_{10} = 2.85 \times 10^{-15}$ s^{-1} is the Einstein coefficient of the hyperfine spontaneous transition. $P_{10} = 1.3 \times 10^9 J_\alpha$ is the deexcitation rate of the hyperfine triplet state due to Lyα scattering. J_α is the intensity of Lyα radiation [31,32],

$$J_\alpha = \frac{c(1+z)^2}{4\pi} \int_z^{z_{\rm max}} \frac{\epsilon(\nu', z')}{H(z')} dz', \tag{5}$$

where $\nu' = \nu_\alpha(1+z')/(1+z)$. $\epsilon(\nu', z')$ is the comoving photon emissivity [1,3,31–33]. Theoretically, the star formation affected by dark matter annihilation could influence the Lyα radiation; see, e.g., Refs. [22,34,35]. In this work, we neglect this effect, which will be discussed in detailed in near-future work. In Eq. (3), y_c corresponds to the collision effect between hydrogen, electrons, and protons, and in this work, we adopt the form used in Refs. [22,30,36,37],

$$y_c = \frac{(C_{\rm HH} + C_{\rm eH} + C_{\rm pH})T_\star}{A_{10} T_k}, \tag{6}$$

where $C_{\rm HH,eH,pH}$ are the deexcitation rate and we adopt the forms used in Refs. [30,36].

In general, the most used quantity for the observation of the global 21 cm signal is the brightness temperature T_{21}, which can be written as [21,32]

$$T_{21} = 26(1 - x_e)\left(\frac{\Omega_b h}{0.02}\right)\left(\frac{0.3}{\Omega_m}\right)^{\frac{1}{2}}\left(\frac{1+z}{10}\right)^{\frac{1}{2}} \times \left(1 - \frac{T_{\rm CMB}}{T_s}\right) \text{ mK}, \tag{7}$$

where x_e is the fraction of free electrons.

III. INFLUENCES OF DARK MATTER ANNIHILATION AND THE FIRST STARS ON THE INTERGALACTIC MEDIUM

Dark matter as the main component of the Universe has been confirmed by many observations, while its nature is still unknown. There are many dark matter models, and the most researched one is weakly interacting massive particles (WIMPs) [38–40]. According to the theory, WIMPs could annihilate into normal particles, such as photons, electrons, and positrons. There are interactions between the particles produced by the dark matter annihilation and the particles present in the Universe. These interactions could influence the evolution of the IGM, and the main influences on IGM are heating, ionization, and excitation [21–26]. Including the dark matter annihilation, the changes of the ionization degree (x_e) and the temperature of IGM (T_k) with the time are [21–26]

$$(1+z)\frac{dx_e}{dz} = \frac{1}{H(z)}[R_s(z) - I_s(z) - I_{\rm DM}(z)], \tag{8}$$

$$(1+z)\frac{dT_k}{dz} = \frac{8\sigma_T a_R T_{\rm CMB}^4}{3 m_e c H(z)} \frac{x_e}{1 + f_{\rm He} + x_e}(T_k - T_{\rm CMB}) - \frac{2}{3 k_B H(z)} \frac{K_{\rm DM}}{1 + f_{\rm He} + x_e} + T_k, \tag{9}$$

where $R_s(z)$ and $I_s(z)$ are the standard recombination rate and ionization rate, respectively. $I_{\rm DM}$ and $K_{\rm DM}$ are the ionization rate and heating rate caused by the dark matter annihilation [24–26]. For our purposes, the influences of dark matter annihilation on the evolution of the IGM should be included in order to investigate the changes of T_k with time. In this paper, we follow the methods presented in Refs. [24–26] and modify the public code RECFAST[2] to include the effects of dark matter annihilation. Including

[2] http://camb.info/.

the dark matter annihilation, e.g., at the redshift $z \sim 20$, the kinetic temperature T_k and ionization degree x_e could reach up to $T_k \sim 100$ K and $x_e \sim 0.001$, respectively [21,22,41].

If we do not include the dark matter annihilation, there are several standard processes that could influence the evolution of IGM [1–3,42]. At high redshift, Compton scattering between CMB photons and the free electrons is the main source of heating. After the formation of the first luminous structures, x rays from, e.g., galaxies and quasars are dominant for heating. The luminosity of the x ray is proportional to the star formation rate, which is proportional to the differential increase of the baryon collapse fraction [1–3,42]. The energy deposited in the IGM from x rays can be written as [22,42]

$$\epsilon_X(z) = 1.09 \times 10^{-31} f_X f_\star \left[\frac{\rho_{b,0}(1+z)^3}{M_\odot \mathrm{Mpc}^{-3}}\right] \left|\frac{df_{\mathrm{coll}}(z)}{dt}\right|, \quad (10)$$

where $f_{\mathrm{coll}}(z)$ is the collapse fraction [3,42]. f_X is a correction factor referring to the differences of the x rays between the low and high redshifts. Given the fact that there are a lot of uncertainties for the x rays from the high-redshift objects, f_X is model dependent, and in general $f_X \gtrsim 1$ [42].[3] In this work, we take the conservative and reasonable value as $f_X = 1$. $f_\star$ is the star formation efficiency and is model dependent. In Ref. [44], the authors found that the star formation efficiency is $f_\star \sim 0.001$–0.01 for normal spiral galaxies and $f_\star \sim 0.01$–0.1 for starburst galaxies, respectively. In this work, we take the conservative value as $f_\star = 0.001$ [42,44,45]. The intensity of Lyα radiation from the x rays can be written as [1,46]

$$J_{\alpha,X} = \frac{c}{4\pi} \frac{1}{H(z)\nu_\alpha} \frac{\epsilon_X}{h\nu_\alpha}. \quad (11)$$

The scattering between the neutral hydrogen atoms and the photons in the Lyman-series resonances could also heat the IGM. In Refs. [31,47], the authors found that the energy deposition rate of this process is very small, and we neglect this process in this work. Another heating source is the shocks in the IGM, and the shock heating is also model dependent. In Ref. [3], the authors found that the effects of shock heating on the IGM are $\lesssim 10\%$. In this work, we do not include this process.

The evolution of T_s and T_k with and without dark matter annihilation is shown in Fig. 1. For comparison, the evolution of T_s, T_k, and T_{CMB} without the influences of reionization sources is also shown (thin solid black lines). Compared with the case without reionization sources, the temperature of IGM increases after the redshift $z \sim 20$ due to the presence of the heating sources. The spin temperature

[3]For some models, f_X could be smaller than unit, $f_X \sim 0.2$ [42,43].

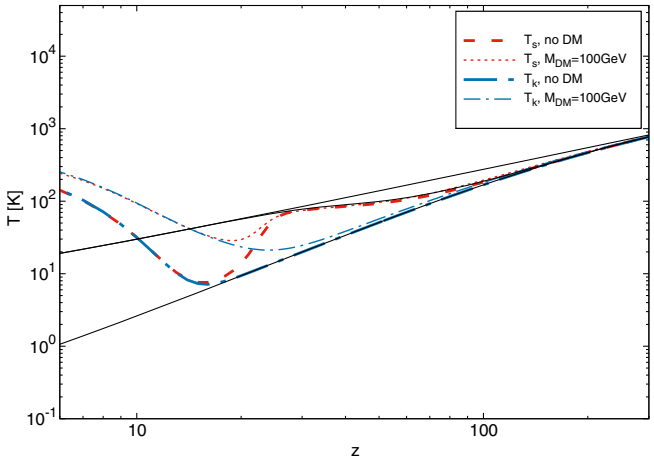

FIG. 1. The evolution of temperature T_s and T_k for the cases with and without dark matter. For comparison, the evolution of T_s, T_k, and T_{CMB} for the case without reionization sources is also shown (thin solid black lines). Here, we set the parameters of dark matter as $M_{\mathrm{DM}} = 100$ GeV and $\langle\sigma \mathrm{v}\rangle = 3 \times 10^{-26}$ cm^{-3} s^{-1}.

T_s decouples from T_k at the redshift $z \sim 200$ and is coupled to T_k again after the redshift $z \sim 20$. The evolution of y_α with time is shown in Fig. 2. One of the factors that could influence y_α is the intensity of the Lyα radiation. In Ref. [22], the authors investigated the evolution of J_α for the cases with and without dark matter annihilation (Fig. 5 in Ref. [22]). It was found that the Lyα background is mainly from the dark matter annihilation during the dark ages, while the contributions from the first stars are dominant after the redshift $z \sim 30$. In Fig. 2, it can be seen that, due to the dark matter annihilation, the values of y_α are larger than that of without dark matter at early times, while the strong gas heating effect reduces the values of y_α after the redshift $z \sim 30$. One should notice that the

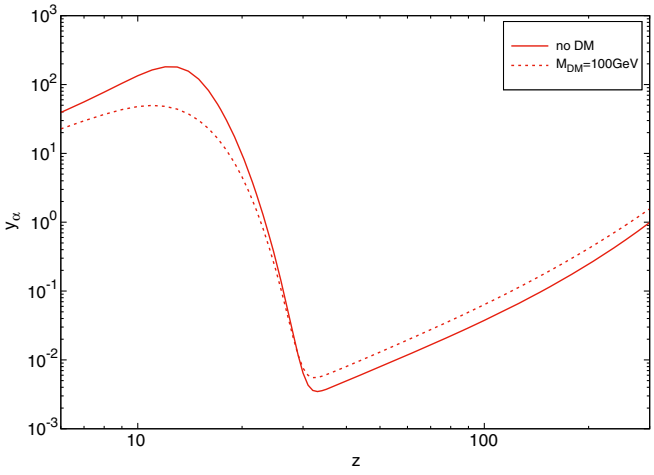

FIG. 2. The evolution of y_α for the cases with and without dark matter. Here, we set the parameters of dark matter as $M_{\mathrm{DM}} = 100$ GeV and $\langle\sigma \mathrm{v}\rangle = 3 \times 10^{-26}$ cm^{-3} s^{-1}.

evolution of T_s and T_k is model dependent, and for detailed discussions, one can refer to, e.g., Refs. [3,21,42].

IV. GLOBAL 21 CM SPECTRUM INCLUDING THE EXCESS OF THE COSMIC RADIO BACKGROUND

As shown in the above section, the temperature of IGM increases due to the dark matter annihilation. Therefore, the observed large amplitude in the global 21 cm spectrum could not be explained easily if the dark matter annihilation were included. In this section, we show that the observed large amplitude in the global 21 cm spectrum could still be explained even including the dark matter annihilation if the excess of the cosmic radio background is included.

As mentioned in Sec. I, the excess of the cosmic radio background in the frequency $\nu \lesssim 1$ GHz has been observed by the ARCADE-2 experiment. The excess could not be explained easily by the standard sources, such as the galactic emission or extragalactic sources counts [17,48]. In Ref. [49], the authors found that the radio excess could be explained in the presence of the magnetic turbulence and shocks in merging galaxy clusters, where the nonthermal electrons are reaccelerated via Alfvén waves. Other possible sources of the radio excess would be from the high-redshift objects. Considering the uncertainties of the radio sources in early times, the excess fraction of the radio background at the high redshift would be small. Moreover, at the high redshift, including the radio excess, the intensity of the radio radiation background would be larger than that of CMB at a rest wavelength of 21 cm [10]. Therefore, following Ref. [10], we write the corresponding temperature of the radio radiation background as

$$T_{\rm CMB}(\nu) = T_0 + \beta T_e \left(\frac{\nu}{1\ {\rm GHz}}\right)^{\alpha}, \qquad (12)$$

where β is a free parameter describing the excess fraction of the cosmic radio background at early times. For our purposes, we set $\nu = 1420\ {\rm MHz}/(1+z)$. It should be noticed that one should use the form $T_{\rm CMB} = T_{\rm CMB}(\nu)(1+z)$ to calculate the brightness temperature T_{21} in Eq. (7).

The global 21 cm spectrum in the redshift $10 \lesssim z \lesssim 30$ is shown in Fig. 3. For our calculations, we set the thermally averaged cross section of dark matter annihilation as $\langle\sigma{\rm v}\rangle = 3\times10^{-26}\ {\rm cm^{-3}\ s^{-1}}$. As shown in Fig. 1, the kinetic temperature T_k is enhanced in the presence of dark matter annihilation after the redshift $z \sim 30$. For the coupling factor y_α, it is depressed for the case of dark matter annihilation after the redshift $z \sim 30$. Therefore, the large absorption feature in the global 21 cm spectrum could not be explained easily if the dark matter annihilation were included. From Fig. 3, it can be seen that, including the excess of the cosmic radio background, the large absorption amplitude could appear in the presence of dark matter annihilation. The absorption amplitude of the global 21 cm spectrum could reach up to $T_{21} \sim 550$ mK at the redshift

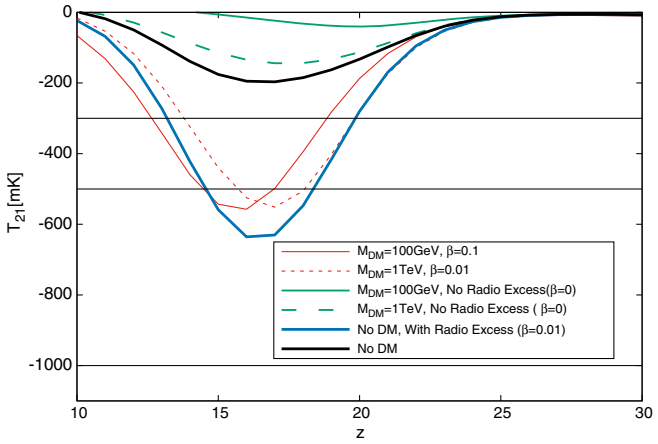

FIG. 3. The global 21 cm spectrum in the redshift $10 \le z \le 30$ including the dark matter annihilation and the excess of the cosmic radio background. Here, we set the thermally averaged cross section of dark matter annihilation as $\langle\sigma{\rm v}\rangle = 3\times10^{-26}\ {\rm cm^{-3}\ s^{-1}}$ and the mass of dark matter particle and the parameter β as $M_{\rm DM} = 100$ GeV, $\beta = 0.1$ (solid red thin line); $M_{\rm DM} = 1$ TeV, $\beta = 0.01$ (dotted red thin line). For comparison, we also show the global 21 cm spectrum for (i) the case without dark matter (solid black bold line); (ii) the case without the excess of the cosmic radio background ($\beta = 0$), $M_{\rm DM}$= 100 GeV (solid green bold line) and $M_{\rm DM}$= 1 TeV (dashed green bold line); and (iii) the case without dark matter but with the excess of the cosmic radio background ($\beta = 0.01$, solid blue bold line). The horizontal lines correspond to the temperature of the global 21 cm spectrum observed by EDGES experiments, $T_{21} = -500^{+200}_{-500}$ mK [4,27].

$z \sim 16$ for $M_{\rm DM} = 100$ GeV and $\beta = 0.1$ (solid red thin line). For $M_{\rm DM} = 1$ TeV and $\beta = 0.01$ (dotted red thin line), the comparable absorption amplitude of the global 21 cm signal appears at the redshift $z \sim 17$. For comparison, we also show the global 21 cm spectrum for (i) the case without dark matter (solid black bold line), (ii) the case without dark matter but with the radio excess (solid blue line), and (iii) the case without the radio excess but with dark matter annihilation (solid and dashed green bold lines). It can be seen that the amplitude of the global 21 cm spectrum decreases for the case with dark matter annihilation. Similar effects could also be found, e.g., in Refs. [21,22,37]. As mentioned in Sec. II, shocks in the IGM could also be a heating source. The amplitude of the global 21 cm signal would be decreased about $\lesssim$10% if shocking heating is included.

One issue that should be noticed is that the dark matter particle with a mass $M_{\rm DM} \sim 1$ TeV could also be used to explain the excess of the positrons flux observed by the DAMPE and AMS-2 experiments [50–53]. On the other hand, the dark matter annihilation has influences on the anisotropy of the cosmic microwave background [24,25,54], and the main influences are on the thermal and reionization history of the IGM. Therefore, the constraints on the parameters of dark matter could be obtained from the

observational results, e.g., the Planck data. In Ref. [54], the authors have the constraints on the dark matter parameters as $M_{\rm DM} \gtrsim 20\,{\rm GeV}$ for $\langle \sigma {\rm v} \rangle = 3 \times 10^{-26}\,{\rm cm}^{-3}\,{\rm s}^{-1}$. Therefore, the parameters of the dark matter used here are within the current allowed parameter space.

Another issue that should be noticed is that the electrons and positrons from the dark matter annihilation could emit the synchrotron radiation in the magnetic field of the Universe. This radiation could contribute to the excess of the cosmic radio background in the frequency $\nu \lesssim 1$ GHz, which has been observed by the ARCADE-2 experiment [18–20,55]. In Refs. [18,19], the authors found that the excess of the cosmic radio background could be explained by the dark matter annihilation, e.g., with the dark matter mass $M_{\rm DM} \sim 20$ GeV and the thermally averaged cross section $\langle \sigma {\rm v} \rangle = 3 \times 10^{-26}\ {\rm cm}^{-3}\,{\rm s}^{-1}$ for the $\mu^+\mu^-$ channel. At early times, the contributions of the dark matter annihilation to the cosmic radio background should be smaller compared to the standard sources such as the radio-loud quasars [16], since the cosmic magnetic field is very weak, $B \lesssim 1$ nG.[4]

In brief, we have considered the popular dark matter annihilation model. The dark matter annihilation has influences on the evolution of the Universe. One of the influences is heating the IGM. Therefore, the absorption amplitude in the global 21 cm spectrum could be reduced or washed out if the dark matter annihilation were included. To explain the observational results of the EDGES experiment, one of the methods is enhancing the cosmic radio background. By considering the excess of the cosmic radio background at high redshift, the heating effects of dark matter annihilation could be weakened. On the other hand, if there is a large radio excess at high redshift, the absorption amplitude in the global 21 cm spectrum could be very large. For this case, the dark matter annihilation could provide a kind of way of pulling the amplitude back.[5]

V. CONCLUSION

Recently, the EDGES experiment has reported a large absorption amplitude in the global 21 cm spectrum. One possible way of explaining the results is decreasing the kinetic temperature. Therefore, it seems that the observed results could not be explained easily if the dark matter annihilation is included due to its heating effects on the IGM. In this work, we have proposed that by considering the excess of the cosmic radio background at early times, although the dark matter annihilation could increase the kinetic temperature, the large absorption amplitude in the global 21 cm spectrum could also be produced. For example, for dark matter mass $M_{\rm DM} = 1$ TeV and ∼1% excess of the cosmic radio background, the absorption amplitude of the global 21 cm spectrum could reach up to $T_{21} \sim 550$ mK at the redshift $z \sim 17$.

The excess of the cosmic radio background reported by the ARCADE-2 experiment cannot be explained easily by the standard sources. The radio excess would be contributed (all or partly) by the redshifted radiation produced at high redshift. Since the dark matter could annihilate into electrons, it is naturally expected that the synchrotron radiation from these electrons could contribute to the excess of the cosmic radio background. In Refs. [18,19], authors found that the radio excess can be explained by the dark matter annihilation. However, one should notice that the contributions of the radio radiation from the dark matter annihilation are mainly from the late times when the intensity of the cosmic magnetic field is large [19]. At high redshift, the contributions of dark matter annihilation to the cosmic radio background would be limited for the standard dark matter halos, because the cosmic magnetic field is weak. However, other astrophysical sources such as the radio-loud quasars could be the sources of the cosmic radio background excess.

In conclusion, we have shown that the popular dark matter annihilation model still works to explain the surprisingly large absorption amplitude of the global 21 cm spectrum in the presence of the cosmic radio background excess, which could be caused by astrophysical sources such as the radio-loud quasars. There are some other different effects that could influence our final results, such as the effects of different dark matter annihilation models on the structure formation, the evolution of IGM, and the Lyα radiation. In theory, the constraints on the dark matter model, such as the lower limit constraints on the dark matter mass, could be obtained from the observational results of the EDGES experiment. Moreover, for the small dark matter mass, even including 100% of the cosmic radio background excess, it is still not possible to explain the large absorption amplitude in the global 21 cm spectrum, because the heating effect from dark matter annihilation is too strong. More detailed calculations and possible constraints on the different dark matter models will be given in near-future work.

ACKNOWLEDGMENTS

We thank Dr. Bin Yue, Xiaoyuan Huang, Lei Feng, Qiang Yuan, and Professor Yizhong Fan for very useful discussions and comments. We also thank the anonymous referees for the very useful comments and suggestions. This work is supported in part by the National Natural Science Foundation of China (under Grants No. 11505005 and No. U1404114).

[4]This value is much smaller than that of the present, $B \sim 1\ \mu$G.

[5]In general, the dark matter annihilation can be neglected, and only the radio excess is included. The large absorption amplitude in the global 21 cm spectrum could also be produced [10]. However, because there is no observational evidence that the dark matter cannot annihilate, it is interesting and worth it to include the dark matter annihilation during the evolution of the Universe.

[1] J. R. Pritchard and A. Loeb, Rep. Prog. Phys. **75**, 086901 (2012).
[2] M. F. Morales and J. S. B. Wyithe, Annu. Rev. Astron. Astrophys. **48**, 127 (2010).
[3] S. Furlanetto, S. P. Oh, and F. Briggs, Phys. Rep. **433**, 181 (2006).
[4] J. D. Bowman, A. E. E. Rogers, R. A. Monsalve, T. J. Mozdzen, and N. Mahesh, Nature (London) **555**, 67 (2018).
[5] R. Barkana, Nature (London) **555**, 71 (2018).
[6] J. B. Muoz and A. Loeb, Nature (London) **557**, 684 (2018).
[7] A. Fialkov, R. Barkana, and A. Cohen, Phys. Rev. Lett. **121**, 011101 (2018).
[8] R. Barkana, N. J. Outmezguine, D. Redigolo, and T. Volansky, arXiv:1803.03091.
[9] S. Fraser *et al.*, Phys. Lett. B **785**, 159 (2018).
[10] C. Feng and G. Holder, Astrophys. J. **858**, L17 (2018).
[11] A. Ewall-Wice, T. C. Chang, J. Lazio, O. Dore, M. Seiffert, and R. A. Monsalve, Astrophys. J. (to be published), arXiv:1803.01815.
[12] D. J. Fixsen, A. Kogut, S. Levin, M. Limon, P. Lubin, P. Mirel, M. Seiffert, J. Singal, E. Wollack, T. Villela, and C. A. Wuensche, Astrophys. J. **734**, 5 (2011).
[13] M. Seiffert, D. J. Fixsen, A. Kogut, S. M. Levin, M. Limon, P. M. Lubin, P. Mirel, J. Singal, T. Villela, E. Wollack, and C. A. Wuensche, arXiv:0901.0559.
[14] A. Kogut, D. J. Fixsen, S. M. Levin, M. Limon, P. M. Lubin, P. Mirel, M. Seiffert, J. Singal, T. Villela, E. Wollack, and C. A. Wuensche, Astrophys. J. **734**, 4 (2011).
[15] J. Singal, Stawarz, A. Lawrence, and V. Petrosian, Mon. Not. R. Astron. Soc. **409**, 1172 (2010).
[16] F. Bolgar, E. Eames, C. Hottier, and B. Semelin, Mon. Not. R. Astron. Soc. **478**, 5564 (2018).
[17] J. Singal *et al.*, Publ. Astron. Soc. Pac. **130**, 036001 (2018).
[18] N. Fornengo, R. Lineros, M. Regis, and M. Taoso, Phys. Rev. Lett. **107**, 271302 (2011).
[19] N. Fornengo, R. Lineros, M. Regis, and M. Taoso, J. Cosmol. Astropart. Phys. 03 (**2012**) 033.
[20] Y. Yang, G. Yang, X. Huang, X. Chen, T. Lu, and H. Zong, Phys. Rev. D **87**, 083519 (2013).
[21] D. T. Cumberbatch, M. Lattanzi, and J. Silk, Phys. Rev. D **82**, 103508 (2010).
[22] Q. Yuan, B. Yue, X.-J. Bi, X. Chen, and X. Zhang, J. Cosmol. Astropart. Phys. 10 (**2010**) 023.
[23] M. Valdes, A. Ferrara, M. Mapelli, and E. Ripamonti, Mon. Not. R. Astron. Soc. **377**, 245 (2007).
[24] L. Zhang, X. Chen, Y.-A. Lei, and Z.-G. Si, Phys. Rev. D **74**, 103519 (2006).
[25] X. Chen and M. Kamionkowski, Phys. Rev. D **70**, 043502 (2004).
[26] Y. Yang, X. Huang, X. Chen, and H. Zong, Phys. Rev. D **84**, 043506 (2011).
[27] G. D'Amico, P. Panci, and A. Strumia, Phys. Rev. Lett. **121**, 011103 (2018).
[28] A. Berlin, D. Hooper, G. Krnjaic, and S. D. McDermott, Phys. Rev. Lett. **121**, 011102 (2018).
[29] Z. Kang, arXiv:1803.04928.
[30] M. Kuhlen, P. Madau, and R. Montgomery, Astrophys. J. **637**, L1 (2006).
[31] X. Chen and J. Miralda-Escudé, Astrophys. J. **602**, 1 (2004).
[32] B. Ciardi and P. Madau, Astrophys. J. **596**, 1 (2003).
[33] R. Barkana and A. Loeb, Astrophys. J. **626**, 1 (2005).
[34] E. Ripamonti, M. Mapelli, and A. Ferrara, Mon. Not. R. Astron. Soc. **375**, 1399 (2007).
[35] R. J. Smith, F. Iocco, S. C. O. Glover, D. R. G. Schleicher, R. S. Klessen, S. Hirano, and N. Yoshida, Astrophys. J. **761**, 154 (2012).
[36] H. Liszt, Astron. Astrophys. **371**, 698 (2001).
[37] Y. Yang, Eur. Phys. J. Plus **131**, 432 (2016).
[38] G. Jungman, M. Kamionkowski, and K. Griest, Phys. Rep. **267**, 195 (1996).
[39] G. Bertone, D. Hooper, and J. Silk, Phys. Rep. **405**, 279 (2005).
[40] X.-J. Bi, P.-F. Yin, and Q. Yuan, Front. Phys. **8**, 794 (2013).
[41] M. Valdés, C. Evoli, A. Mesinger, A. Ferrara, and N. Yoshida, Mon. Not. R. Astron. Soc. **429**, 1705 (2013).
[42] S. Furlanetto, Mon. Not. R. Astron. Soc. **371**, 867 (2006).
[43] S. C. O. Glover and P. W. J. L. Brand, Mon. Not. R. Astron. Soc. **340**, 210 (2003).
[44] K. Wada and C. Norman, Astrophys. J. **660**, 276 (2007).
[45] N. Y. Gnedin, Astrophys. J. **535**, 530 (2000).
[46] X.-L. Chen and J. Miralda-Escude, Astrophys. J. **684**, 18 (2008).
[47] G. B. Rybicki, Astrophys. J. **647**, 709 (2006).
[48] N. Fornengo, R. A. Lineros, M. Regis, and M. Taoso, J. Cosmol. Astropart. Phys. 04 (**2014**) 008.
[49] K. Fang and T. Linden, J. Cosmol. Astropart. Phys. 10 (2016) 004.
[50] G. Ambrosi *et al.* (DAMPE Collaboration), Nature (London) **552**, 63 (2017).
[51] G. H. Duan, L. Feng, F. Wang, L. Wu, J. M. Yang, and R. Zheng, J. High Energy Phys. 02 (2018) 107.
[52] L. Zu, C. Zhang, L. Feng, Q. Yuan, and Y.-Z. Fan, Phys. Rev. D **98**, 063010 (2018).
[53] Q. Yuan *et al.*, arXiv:1711.10989.
[54] Y. Yang, Phys. Rev. D **91**, 083517 (2015).
[55] J. Singal, D. J. Fixsen, A. Kogut, S. Levin, M. Limon, P. Lubin, P. Mirel, M. Seiffert, T. Villela, E. Wollack, and C. A. Wuensche, Astrophys. J. **730**, 138 (2011).